

Excited states of the quasi-one-dimensional hexagonal quantum antiferromagnets

M. Merdan^{1,2} and Y. Xian¹

¹*School of Physics and Astronomy, The University of Manchester, Manchester M13 9PL, UK*

²*Department of Physics, College of Science, University of Babylon, Babylon, Iraq*

(Dated: June 22, 2022)

We investigate the excited states of the quasi-one-dimensional quantum antiferromagnets on hexagonal lattices, including the longitudinal modes based on the magnon-density waves. A model Hamiltonian with a uniaxial single-ion anisotropy is first studied by a spin-wave theory based on the one-boson method; the ground state thus obtained is employed for the study of the longitudinal modes. The full energy spectra of both the transverse modes (i.e., magnons) and the longitudinal modes are obtained as functions of the nearest-neighbor coupling and the anisotropy constants. We have found two longitudinal modes due to the non-collinear nature of the triangular antiferromagnetic order, similar to that of the phenomenological field theory approach by Affleck. The excitation energy gaps due to the anisotropy and the energy gaps of the longitudinal modes without anisotropy are then investigated. We then compare our results for the longitudinal energy gaps at the magnetic wavevectors with the experimental results for several antiferromagnetic compounds with both integer and non-integer spin quantum numbers, and we find good agreement after the higher-order contributions are included in our calculations.

PACS numbers: 75.10.Jm, 75.30.DS, 75.50.Ee.

I. INTRODUCTION

The excitations of the quasi-one-dimensional (1d) Heisenberg antiferromagnets systems have been studied extensively since Haldane predicted an energy gap in the excitation spectra of the isotropic *integer*-spin Heisenberg chains in 1983 [1]. Now it is well established that there is an energy gap separating the singlet ground state from the triplet lowest-energy-excitation states for the *integer*-spin Heisenberg chains, contrast to the gapless excitation states of the *half-odd-integer*-spin Heisenberg systems [2, 3]. This theoretical prediction has been confirmed by Buyers *et al* [4] in the inelastic-neutron-scattering experiments on the quasi-1D antiferromagnetic compound CsNiCl₃. Some subsequent experimental investigations [4–8] and numerical calculations [9–13] also support Haldane’s prediction.

At very low temperature, most of the quasi-1D antiferromagnetic materials including CsNiCl₃ show the three-dimensional nature with the classical magnetic order, and more interestingly, energy gaps at the magnetic wavevector have also been observed in many compounds [4]. For the case of CsNiCl₃, the observed energy gap was initially explained by a uniaxial single-ion anisotropy but now it is widely accepted that the gapped excited state belongs to one of the two longitudinal modes corresponding to the oscillations in the magnitude of the magnetic order of the quasi-1D hexagonal systems, first proposed by Affleck based on a simplified version of Haldane’s theory [14, 15]. The gapped longitudinal modes are clearly beyond the conventional spin-wave theory which produces only the transverse excitations usually referred to as magnons. A Later experimental study by Enderle *et al.* [16] using high-resolution polarized neutron scattering also confirms Affleck’s proposal of the longitudinal modes, and contradicts the spin-wave theory of two-magnon by Ohyama and Shiba [17] or a modified spin-wave theory by Plumer and Caillé [18]. There are also investigations of the longitudinal excitation states in other quasi-1D structures with the Néel-like long-ranged order at low temperature such as the

tetragonal KCuF₃ with $s = 1/2$ [19], where good agreements between the experiment and a theory based on a sine-Gordon field theory have been found for the energy gap at the magnetic wavevector [20, 21]. More recently, a longitudinal mode was also observed in the dimerized antiferromagnetic compound TiCuCl₃ under pressure with a long-ranged Néel order [22].

We recently proposed a general microscopic many-body theory based on the magnon-density waves for the longitudinal excitations of spin- s quantum antiferromagnetic systems [23, 24]. In analogy to Feynmann’s theory of the low-lying excited states in the helium-4 superfluid [25, 26], we identify the longitudinal excitation states in a quantum antiferromagnet with a Néel-like order as the collective modes of the magnon-density waves. In application to the quasi-1D tetragonal structure of KCuF₃ with $s = 1/2$, with no other fitting parameters than the nearest-neighbor coupling constants in the model Hamiltonian, we find that our numerical results for the energy gap values at the magnetic wavevector are in general agreement with the experiments [27]. We hope that more experimental results for the energy spectra at other wavevectors will be available for comparison.

In this article, we extend our microscopic approach to the quasi-1D hexagonal quantum antiferromagnets such as CsNiCl₃ and RbNiCl₃ [16, 28, 29] both with spin-1 and CsMnI₃ with spin-5/2 [30]. Furthermore, we also investigate the higher-order contributions to the longitudinal excitation spectra in the large- s expansion. The basal planes of these materials are antiferromagnetic triangular lattice with the noncollinear magnetic order. Hence there are two possible longitudinal modes in these hexagonal systems, rather than the single longitudinal mode of the bipartite systems such as the tetragonal KCuF₃. Some preliminary results for the two dimensional triangular model have been published [31]. We organize this article as follows. For completeness, we outline the main results of the spin-wave theory for the quasi-1D model in Sec. II, using the one-boson approach after two spin rotations. We obtain the full spin-wave spectra as a func-

tion of the uniaxial single-ion anisotropy. To our knowledge, this anisotropy dependence of the spin-wave spectra has not been published before. We then apply our microscopic theory for the longitudinal excitations in Sec. III, using the approximated ground state from the spin-wave theory. The energy gaps due to the anisotropy and the energy gaps of the longitudinal modes without anisotropy are then discussed in details. We compare our results for the longitudinal energy gaps with the experimental results for the spin-1 compounds CsNiCl₃ and RbNiCl₃ and the spin-5/2 compound CsMnI₃. We find good agreements for the energy gap values for CsNiCl₃ and RbNiCl₃ after including the higher-order contributions in our calculations. For CsMnI₃ which is very close to the pure 1d system we find a big discrepancy between our approximation of the gap value and the experimental results. We conclude this article by a summary and a discussion of the possible further corrections particularly for CsMnI₃.

II. THE SPIN-WAVE THEORY OF THE ANISOTROPIC HEXAGONAL ANTIFERROMAGNETIC SYSTEMS

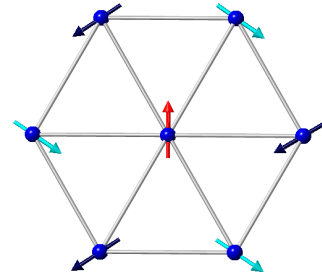
The quasi-1D materials such as CsNiCl₃ crystallize in the hexagonal ABX_3 structure with space group $P6_3/mmc$, where A is an alkaline-metal cation, B is a cation of the $3d$ group, and X is a halogen anion. The magnetic ions B constructs the hexagonal lattice in the ab plane with adjacent spins forming angles of $\theta = 2\pi/3$, and antiparallel adjacent spins along the chain of the c axis as shown in Figs. 1(a) and (b). The lattice constants of CsNiCl₃, for example, are $a = 7.14$ Å and $c = 5.90$ Å, and the magnetic moments are carried by Ni²⁺. The superexchange interaction between B (Ni²⁺) ions is modeled by an N -spin Heisenberg Hamiltonian with a strong intrachain interaction J and weak interchain interaction J' such as

$$H = 2J \sum_{\langle i,j \rangle}^{\text{chain}} \mathbf{S}_i \cdot \mathbf{S}_j + 2J' \sum_{\langle i,j \rangle}^{\text{plane}} \mathbf{S}_i \cdot \mathbf{S}_j + D \sum_i (S_i^z)^2, \quad (1)$$

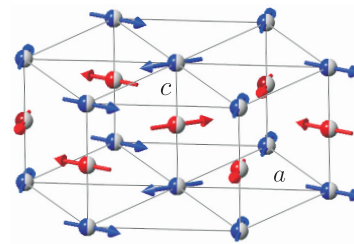
where the notation $\langle i,j \rangle$ indicates the nearest-neighbor couplings only and where we have also added an Ising-like single-ion anisotropy term with constant $D (< 0)$. Most of the intrachain couplings in ABX_3 compounds are antiferromagnetic such as in CsNiCl₃ or RbNiCl₃ with easy single-site anisotropy, or CsMnBr₃ and RbMnBr₃ with hard anisotropy [32, 33]. These intrachain couplings can also be ferromagnetic (i.e., $J < 0$) as in CsNiF₃ [34, 35] or CsCuCl₃ [36]. We consider only the antiferromagnetic couplings here. Therefore, the classical ground state of each linear chain along the c axis (also denoted as y -axis) is a Néel state with alternating spin-up (blue) and spin-down (red) alignments as shown in Fig. 1 (b).

We consider a spin-wave theory for the Hamiltonian (1) based on the one-boson approach by performing two spin rotations. Firstly, we rotate the local axes of all up-spins (blue) by 180° so that all spins along each chain align in the same down direction. This is equivalent to the transformation

$$S_i^{\mp} \rightarrow -S_i^{\pm}, \quad S_i^z \rightarrow -S_i^z \quad (2)$$



(a)



(b)

FIG. 1. (Color online) The classical spin structure of the quasi-1D hexagonal antiferromagnets: (a) on the ab plane, and (b) the three-dimensional structure.

for the first terms in Eq. (1), leaving the last two terms unchanged. The second rotation is on the hexagonal lattice of the ab plane (or xz -plane) on the second and third terms of Eq. (1). Following Singh and Huse [37] and Miyake [38], for every triangle of the hexagonal lattices [see Fig 1(a)], we rotate the local axes of two spins along the classical direction in the xz -plane to align with that of the third spin [39, 40]. This is equivalent to the rotation of the i -sites of Eq. (1) by the following transformation

$$\begin{aligned} S_i^x &\rightarrow S_i^x \cos(\theta_i) + S_i^z \sin(\theta_i), \\ S_i^y &\rightarrow S_i^y, \\ S_i^z &\rightarrow S_i^z \cos(\theta_i) - S_i^x \sin(\theta_i), \end{aligned} \quad (3)$$

where $\theta_i \equiv \mathbf{Q}_z \cdot \mathbf{r}_i$ and $\mathbf{Q}_z = (4\pi/3, 0, q_z)$ with \mathbf{Q}_z at $q_z = \pi$ defined as the magnetic-ordering wavevector of the quasi-1D hexagonal systems. The Hamiltonian (1) after these two transformations is given as

$$H = -\frac{1}{2}J \sum_{l,\varrho}^{\text{chain}} [S_l^+ S_{l+\varrho}^+ + S_l^- S_{l+\varrho}^- + 2S_l^z S_{l+\varrho}^z] - \frac{1}{2}J' \sum_{l,\varrho'}^{\text{plane}} [S_l^z S_{l+\varrho'}^z + \frac{3}{4}(S_l^+ S_{l+\varrho'}^+ + S_l^- S_{l+\varrho'}^-) - \frac{1}{4}(S_l^+ S_{l+\varrho'}^- + S_l^- S_{l+\varrho'}^+) - 2\sin(\theta_l - \theta_{l+\varrho'})(S_l^z S_{l+\varrho'}^x - S_l^x S_{l+\varrho'}^z)] + \tilde{\mathcal{H}}^D, \quad (4)$$

where l runs through all sites, ϱ and ϱ' are the nearest neighbor index vectors with coordination numbers $z = 2$ along the chain and $z' = 6$ on the hexagonal basal planes respectively, and $\tilde{\mathcal{H}}^D$ is the rotated anisotropy term. Care should be taken for the two rotations on this anisotropy term. The first rotation of Eq. (2) leaves it unchanged due to its quadratic form as mentioned before. In order to perform the second rotation of Eq. (3) involving rotations of the axes of the two spins to align with the axis of the third spin on the triangular planes, we rewrite the anisotropy term of Eq. (1) in the following equivalent, suitable form

$$\sum_i (S_i^z)^2 = \frac{1}{z'} \sum_{l,\varrho'} \left[\frac{1}{3}(S_l^z)^2 + \frac{2}{3}(S_{l+\varrho'}^z)^2 \right]. \quad (5)$$

The transformation of Eq. (3) to the second term in Eq. (5) gives

$$\begin{aligned} \tilde{\mathcal{H}}^D = & \frac{1}{z'} \sum_{l,\varrho'} \left[\frac{1}{3}D(S_l^z)^2 + \frac{2}{3}D[(S_{l+\varrho'}^z)^2 \cos^2 \theta_{l+\varrho'} \right. \\ & \left. + (S_{l+\varrho'}^x)^2 \sin^2 \theta_{l+\varrho'} - \cos \theta_{l+\varrho'} \sin \theta_{l+\varrho'} (S_{l+\varrho'}^z S_{l+\varrho'}^x \right. \\ & \left. + S_{l+\varrho'}^x S_{l+\varrho'}^z) \right]. \end{aligned} \quad (6)$$

We notice that this anisotropy form is different from the simple form of Ref. [43] or that of Ref. [44]. We believe that Eq. (6) is the correct form suitable for the hexagonal systems. The energy gaps in the energy spectra due to this anisotropy term will be presented later.

Using the canonical Holstein-Primakoff transformations, the spin operators are expressed in terms of a single set of boson operators a^\dagger and a as,

$$S^+ = \sqrt{2s}fa, \quad S^- = \sqrt{2s}a^\dagger f, \quad S^z = s - a^\dagger a, \quad (7)$$

where $f = \sqrt{1 - a^\dagger a/2s}$ and s is the spin quantum number. The Hamiltonian of Eq. (4) can then be written as, after Fourier transformations of the boson operators with the Fourier component operators a_q and a_q^\dagger and to the order of $(2s)$,

$$H \approx H_0 + H_2, \quad (8)$$

where H_0 is the classical energy,

$$H_0 = -2JNs^2 - 3J'Ns^2 + \frac{1}{3}DNs^2(1 + 2\cos^2 \theta + \frac{1}{s}\sin^2 \theta) \quad (9)$$

with $\theta = 2\pi/3$ and H_2 is given by the quadratic terms in the boson operators as

$$H_2 = s \sum_q [A_q a_q^\dagger a_{-q} - \frac{1}{2}B_q (a_q^\dagger a_{-q}^\dagger + a_q a_{-q})] \quad (10)$$

with constants A_q and B_q defined by

$$\begin{aligned} A_q &= 4J + 6J'(1 + \frac{1}{2}\gamma_q) - \frac{2}{3}D(1 + 2\cos^2 \theta - \sin^2 \theta), \\ B_q &= 4J \cos q_z + 9J'\gamma_q - \frac{2}{3}D \sin^2 \theta, \end{aligned} \quad (11)$$

and γ_q defined as usual by

$$\gamma_q = \frac{1}{z'} \sum_{\varrho'} e^{i\mathbf{q}\cdot\mathbf{r}_{\varrho'}} = \frac{1}{3} \left(\cos q_x + 2 \cos \frac{q_x}{2} \cos \frac{\sqrt{3}}{2} q_y \right). \quad (12)$$

The quadratic Hamiltonian H_2 of Eq. (10) is diagonalized by the usual Bogoliubov transformation and can be written in terms of the new boson operators α_q and α_q^\dagger as,

$$H_2 = \Delta H_0 + \sum_q \mathcal{E}_q \left(\alpha_q^\dagger \alpha_q + \frac{1}{2} \right), \quad (13)$$

where ΔH_0 is the quantum correction to the classical ground state energy of Eq. (9),

$$\Delta H_0 = -2JNs - 3J'Ns + \frac{1}{3}DNs(1 + 2\cos^2 \theta - \sin^2 \theta), \quad (14)$$

and \mathcal{E}_q is the spin-wave excitation spectra,

$$\mathcal{E}_q = s \sqrt{A_q^2 - B_q^2}. \quad (15)$$

The first Brillouin zone of a quasi-1D antiferromagnet is plotted in Fig. 2, where the magnetic wavevector $\mathbf{Q} = (4\pi/3, 0, \pi)$ is located at the corner of the hexagon and where other symmetry points in conventional notations are also illustrated. We plot the spin-wave spectra of Eq. (15) in Fig. 3 for CsNiCl₃ using the experimental values $J = 0.345$, $J' = 0.0054$ THz and negligible anisotropy $D \approx 0$ [4, 14, 16, 41, 42]. We define the ratio of the two nearest-neighbor coupling constants as ξ and, for CsNiCl₃,

$$\xi = \frac{J'}{J} = 0.0157. \quad (16)$$

The spin-wave energy spectra with different polarizations are obtained by folding of the wavevectors. In Fig. 3, several branches along the symmetry direction of $(0, 0, \eta + 1)$, $(\eta, \eta, 1)$, and $(1/3, 1/3, 1 + \eta)$ are shown, where η is the reduced wave vector component in the reciprocal lattice unit (r.l.u) with $q_z = (2\pi l/c) \cdot (c/2) = \pi l$, and $\gamma = 1/3[\cos 2\pi h + \cos 2\pi k + \cos 2\pi(h+k)]$. Using Eq. (12) the moving in the

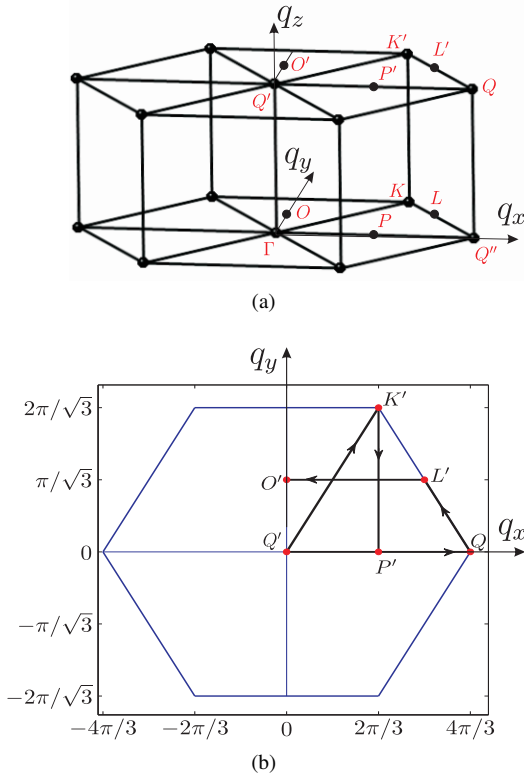


FIG. 2. (a) The first Brillouin zone of a quasi-1D hexagonal antiferromagnets. The points $(0, 0)$, $(2\pi/3, 2\pi/\sqrt{3})$, $(2\pi/3, 0)$, $(4\pi/3, 0)$, $(\pi, \pi/\sqrt{3})$, and $(0, \pi/\sqrt{3})$ all at $q_z = \pi$ are denoted as Q', K', P', Q, L', O' respectively, and the similar points at $q_z = 0$ are denoted as Γ, K, P, Q'', L, O respectively. (b) The hexagonal Brillouin zone at $q_z = \pi$ with some symmetry points in conventional notations for the quasi-1D systems.

paramagnetic Brillouin zone can be written as for $q_x = 4\pi\eta$ and $q_z = \pi + \pi\eta$, and the corresponding symmetry directions to those in reciprocal lattice unit are $(0, 0, \pi + \pi\eta)$, $(4\pi\eta, 0, \pi)$ and $(4\pi/3, 0, \pi + \pi\eta)$ respectively. The three transverse spin-wave branches are obtained from Eq. (15) as follows. The y -mode has the polarization along the y -axis of the hexagonal lattice where the quantum fluctuation is at q ; the other two modes are found in the xz -plane by translating the wavevector by a magnetic wavevector as $q \rightarrow (q \pm Q)$ and are denoted as zx_{\pm} respectively.

As can be seen from Fig. 3, at the magnetic wavevector \mathbf{Q} , the y -mode is gapless for zero anisotropy ($D = 0$). However, as mentioned earlier, an energy gap about $0.41(2J)$ has been observed by the neutron scattering experiments for CsNiCl_3 [4]. This energy gap can be reproduced in the y -mode excitation by introducing an anisotropy with $D = -0.0285$ using our approximation of Eq. (6), also plotted in Fig. 3. If we use the simple form of Ref. [43] corresponding to setting $\theta = 0$ in Eq.(6), the required anisotropy is reduced by a little more than half with the value $D = -0.0141$. Both of these values are now considered too large for CsNiCl_3 which has negligible anisotropy. The conclusion is that the observed gaps are not of the transverse spin-wave spectra, but belong to the lon-

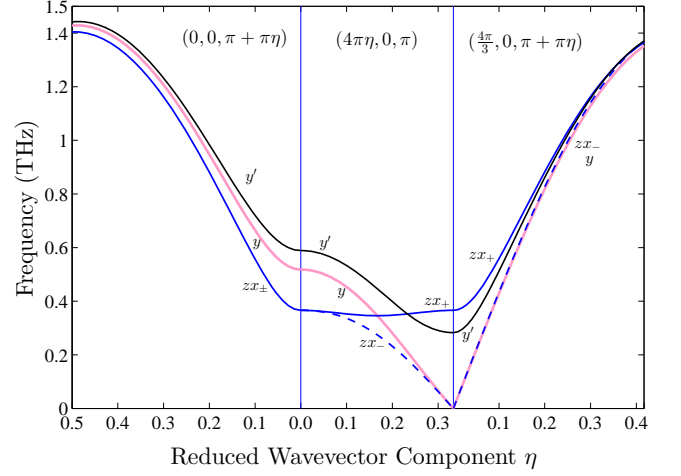


FIG. 3. The three spin-wave excitation spectra (in colors) for CsNiCl_3 with $J = 0.345$, $J' = 0.0054$ and $D = 0$ THz, along the symmetry direction $(0, 0, \pi + \pi\eta)$, $(4\pi\eta, 0, \pi)$ and $(\frac{4\pi}{3}, 0, \pi + \pi\eta)$. Also included is the gapped y -mode (black, denoted as y') with $D = -0.0285$ using the anisotropy term of Eq. (6). The solid and dash with the blue color on the lines indicate the zx_+ -mode and zx_- -mode respectively.

gitudinal modes, as first proposed by Affleck [14, 15].

Now we turn our attention to the order parameter. The long-range order of the quasi-1D hexagonal systems is given by the three sublattice-magnetizations with the same magnitude but different orientations as shown in Fig. 1, and it is clearly noncollinear, contrast to the collinear case of the bipartite systems. In the spin-wave theory with one boson method as described above, the magnitude of the sublattice magnetization can be expressed as

$$M = \frac{1}{N} \sum_l \langle S_l^z \rangle = s - \rho, \quad (17)$$

where the quantum correction ρ is the magnon density defined as the ground-state expectation value of the boson number operator

$$\rho = \langle a_l^\dagger a_l \rangle = \frac{1}{N} \sum_q \frac{1}{2} \left(\frac{A_q}{\sqrt{A_q^2 - B_q^2}} - 1 \right), \quad (18)$$

with A_q and B_q defined by Eqs. (11). The numerical result of the magnon density for CsNiCl_3 is $\rho \approx 0.49$ at $D = 0$, giving the sublattice magnetization $M \approx 0.51$. On the other hand, using slightly different parameter $\xi = 1.7 \times 10^{-2}$ from Ref. [44], we obtain $\rho = 0.48$, giving $M = 0.52$. Both these results compare favorably with the experimental value of $M = 0.53$ [44]. As mentioned earlier, our microscopic analysis of the longitudinal modes is based on these magnon density fluctuations and there will be two such modes as discussed in details in the following section.

III. THE LONGITUDINAL MODES OF THE QUASI-1D HEXAGONAL ANTIFERROMAGNETS

As mentioned before, the longitudinal excitations in a quantum antiferromagnetic system with a Néel-like long-ranged order correspond to the fluctuations in the order parameter. Using the fact that the quantum correction in the order parameter is given by the magnon density ρ as discussed previously in Eq. (17), the longitudinal modes can be considered as the magnon-density waves. By analogy to Feynman's theory on the low-lying excited states of the helium-4 superfluid [25], the longitudinal excitation states can be constructed by employing the magnon-density operators S^z , in contrast the transverse spin-wave excitation states constructed by the spin-flip operators S^\pm [24]. The energy spectra of these longitudinal collective modes can then be easily derived by a formula first employed by Feynman for the famous phonon-roton spectrum of the helium superfluid involving the structure factor of its ground state.

More specifically, following Feynman as described above, the longitudinal excitation state is approximated by applying the magnon density fluctuation operator X_q to the ground state $|\Psi_g\rangle$ as,

$$|\Psi_e\rangle = X_q|\Psi_g\rangle, \quad (19)$$

where X_q is given by the Fourier transformation of S^z operators,

$$X_q = \frac{1}{\sqrt{N}} \sum_l e^{i\mathbf{q}\cdot\mathbf{r}_l} S_l^z, \quad q > 0, \quad (20)$$

with index l running over all lattice sites. The condition $q > 0$ in Eq. (20) ensures the orthogonality to the ground state. The energy spectrum for the trial excitation state of Eq. (19) can be written as

$$E(q) = \frac{\langle\Psi_g|\tilde{X}_q H X_q|\Psi_g\rangle}{\langle\Psi_e|\Psi_e\rangle} - E_g = \frac{\langle\Psi_g|\tilde{X}_q[H, X_q]|\Psi_g\rangle}{\langle\Psi_e|\Psi_e\rangle}$$

where \tilde{X}_q is the Hermitian of X_q and where in the second equation we have used the ground state equation, $H|\Psi_g\rangle = E_g|\Psi_g\rangle$. We notice that operator S_l^z in X_q of Eq. (20) is a Hermitian operator, hence $\tilde{X}_q = X_{-q}$. By considering the similar excitation state $X_{-q}|\Psi_g\rangle$ with the energy spectrum $E(-q) = E(q)$, it is straightforward to derive [24],

$$E(q) = \frac{N(q)}{S(q)}, \quad (21)$$

where $N(q)$ is given by the ground-state expectation value of a double commutator as

$$N(q) = \frac{1}{2} \langle [X_{-q}, [H, X_q]] \rangle_g, \quad (22)$$

and the state normalization integral $S(q)$ is the structure factor of the lattice model

$$S(q) = \langle\Psi_e|\Psi_e\rangle = \frac{1}{N} \sum_{l,l'} e^{i\mathbf{q}\cdot(\mathbf{r}_l - \mathbf{r}_{l'})} \langle S_l^z S_{l'}^z \rangle_g. \quad (23)$$

The notation $\langle \dots \rangle_g$ in Eqs. (22) and (23) indicates the ground-state expectation.

In fact, the excitation state of Eqs. (19) and (20) can also be viewed as the single-mode approximation (SMA) [45] and the expression for $E(q)$ is actually the exact first moment of the dynamic longitudinal structure factor. We also like to point out that the relation between the longitudinal magnon-density waves and the quasiparticle magnon modes can be examined by the first commutation of the operator (20) with the Hamiltonian and that the magnon-density waves represent the coherent motion of the spin ± 1 magnon pairs, very similar to the plasmon excitations in the electronic systems with coherent motion of quasi-electron-hole pairs as discussed in details in our earlier paper [23].

Further support for the form of Eq. (19) can also be obtained by examining the general structures of the ground and excited states within the framework of the coupled-cluster method (CCM) [46–48]. Briefly, within the CCM, the ground state is given by applying an exponentiated correlation operator \hat{S} on a reference state $|\Phi\rangle$ (i.e., the classical Néel state in our case) as

$$|\Psi_g\rangle = e^{\hat{S}}|\Phi\rangle, \quad \hat{S} = \sum_I F_I C_I^\dagger \quad (24)$$

with the multiparticle creation operator C_I^\dagger and the corresponding variational coefficients F_I . In our case here, C_I^\dagger is given by the products of the spin-flip operators S^+ with respect the Néel state. The excitation state within the CCM is given by the linear form as [24, 49, 50]

$$|\Psi_e\rangle = X|\Psi_g\rangle = X e^{\hat{S}}|\Phi\rangle, \quad X = \sum_I x_I C_I^\dagger \quad (25)$$

with the variational coefficients x_I . In fact, the spin-wave ground state as discussed in Sec. II can be deduced by a low-order, the so-called SUB2 approximation involving the two-body correlations, in the large- s limit of the CCM [51]. Furthermore, using the following algebra

$$\begin{aligned} S_l^z e^{\hat{S}} &= e^{\hat{S}} \bar{S}_l^z, \\ \bar{S}_l^z &= e^{-\hat{S}} S_l^z e^{\hat{S}} = S_l^z + [S_l^z, \hat{S}] + \frac{1}{2!} [[S_l^z, \hat{S}], \hat{S}] + \dots \end{aligned}$$

where the nested commutation series in \bar{S}_l^z terminates at the first order in our case, it is not difficult to show the similarity between the excitation state of Eqs. (19-20) and that of Eq. (25). The clear advantage of Eqs. (19) and (20) lies on its simple form and on the fact that the double commutation in $N(q)$ of Eq. (22) reduces the order of calculations. Furthermore, it satisfies the sum rule as described above in the (SMA).

We have applied these formulas to the bipartite quasi-1D antiferromagnetic systems such as KCuF_3 [27]. For the hexagonal lattice systems as discussed here, we expect that there are two longitudinal modes due to the noncollinear nature of the order parameter on the triangular basal plane. Within the one-boson approach after the two spin rotations as employed here, the two longitudinal modes with xz -polarizations of the hexagonal systems can be obtained by

folding of the wavevectors in the energy spectra of Eq. (21), in similar fashion to the one-boson spin-wave theory as discussed in Sec. II and also to that of Ref. [14].

Using the Hamiltonian of Eqs. (4), it is straightforward to derive the following double commutator with zero anisotropy (i.e. $D = 0$) as

$$N(q) = 2sJ \sum_{\rho} (1 + \cos q_z) \tilde{g}_{\rho} + \frac{1}{2} J' s \sum_{\rho'} \left[3(1 + \gamma_q) \tilde{g}'_{\rho'} - (1 - \gamma_q) \tilde{g}'_{\rho'} \right], \quad (26)$$

where γ_q is as defined in Eq. (12) and the transverse correlation functions \tilde{g}_{ρ} and $\tilde{g}'_{\rho'}$ are defined respectively as

$$\tilde{g}_{\rho} = \frac{1}{2s} \langle S_l^+ S_{l+\rho}^+ \rangle_g \quad \tilde{g}'_{\rho'} = \frac{1}{2s} \langle S_l^+ S_{l+\rho'}^- \rangle_g, \quad (27)$$

all independent of index l due to the lattice translational symmetry. Also, the contribution from the three-boson operators with $\sin(\theta_l - \theta_{l+\rho})$ (the so-called cubic term) is zero. We notice that this cubic term has been included in perturbation theory for the correction in spin-wave spectrum [38, 39]. In evaluating \tilde{g}_{ρ} and $\tilde{g}'_{\rho'}$ of Eq. (27), we keep up to the second order in the large- s expansions and obtain

$$\begin{aligned} \tilde{g}_{\rho} &= \Delta_{\rho} - \frac{2\rho \Delta_{\rho} + \mu_{\rho} \delta}{2s}, \\ \tilde{g}'_{\rho'} &= \mu_{\rho'} - \frac{2\rho' \mu_{\rho'} + \Delta_{\rho'} \delta}{2s}, \end{aligned} \quad (28)$$

where

$$\begin{aligned} \rho &= \langle a_l^{\dagger} a_l \rangle = \frac{1}{N} \sum_q \rho_q, \quad \mu_{\rho} = \langle a_l^{\dagger} a_{l+\rho} \rangle = \frac{1}{N} \sum_q e^{i\mathbf{q}\cdot\rho} \rho_q, \\ \Delta_{\rho} &= \langle a_l a_{l+\rho} \rangle = \frac{1}{N} \sum_q e^{i\mathbf{q}\cdot\rho} \Delta_q, \quad \delta = \langle a_l a_l \rangle = \frac{1}{N} \sum_q \Delta_q, \end{aligned} \quad (29)$$

and where

$$\Delta_q = \frac{1}{2} \frac{B_q}{\sqrt{A_q^2 - B_q^2}}, \quad \rho_q = \frac{1}{2} \left(\frac{A_q}{\sqrt{A_q^2 - B_q^2}} - 1 \right), \quad (30)$$

with A_q and B_q as given before by Eqs. (11). The structure factor within the linear spin-wave approximation is independent of s , and is given by

$$S(q) = \rho + \frac{1}{N} \sum_{q'} \rho_{q'} \rho_{q+q'} + \frac{1}{N} \sum_{q'} \Delta_{q'} \Delta_{q+q'}. \quad (31)$$

We like to point out that, the calculations of both Eqs. (28) and (31) involve up to four-boson operators.

We first discuss the general behaviors of the longitudinal spectrum of Eq. (21) as a function of the ratio of the two nearest-neighbor coupling constants, $\xi = J'/J$. In the limit $\xi \rightarrow 0$, the Hamiltonian of (1) becomes the pure 1d systems;

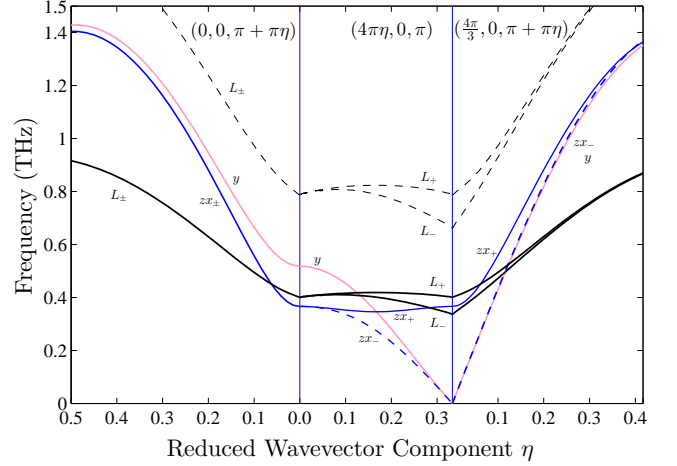


FIG. 4. The longitudinal modes L_{\pm} as derived from Eq. (21) together with the spin-wave y - and zx_{\pm} modes as derived from Eq. (15) for CsNiCl₃ along the symmetry direction $(0, 0, \pi + \pi\eta)$, $(4\pi\eta, 0, \pi)$ and $(\frac{4\pi}{3}, 0, \pi + \pi\eta)$. The longitudinal modes L_{\pm} calculated from the first order approximation and after including the second term in Eq. (28) are indicated by the dash and solid lines respectively.

the longitudinal spectrum is gapless and identical to the doublet spin-wave spectra thus forming a triplet excitation state as discussed in details Ref. [27]. This demonstrates the limitation by the spin-wave ground-state employed, particularly when applied to the integer-spin Heisenberg chain where the Haldane gap is expected as discussed in Sec. I. In the other limit, $\xi \rightarrow \infty$, the Hamiltonian is a pure triangular antiferromagnet with the quasi-gapped longitudinal modes as discussed in details in our previous paper [31] where we keep only the first order term in Eq. (28) in the large s -expansion, similar to the case of the square lattice model.

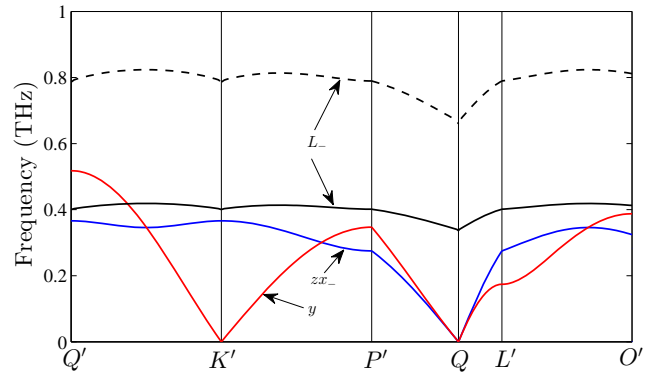


FIG. 5. The longitudinal mode L_{-} along path $Q'K'P'QL'O'$ of the hexagonal Brillouin zone of Fig. 2(b) together with the spin-wave y and zx_{-} modes for CsNiCl₃. The longitudinal modes L_{\pm} calculated from the first order approximation and after including the second term in Eq. (28) are indicated by the dash and solid lines respectively.

For the quasi-1D materials with intermediate values of ξ , the spin-wave ground state is a reasonable approximation. We obtain nonzero energy gaps for the longitudinal excitation spectra of Eq. (21). As discussed before, following Affleck [14, 15], two longitudinal modes for the quasi-1D hexagonal antiferromagnets can be obtained by folding of the wavevector. We denote one as L_- with the spectrum $E(q - Q)$ and the other as L_+ with the spectrum $E(q + Q)$. We plot these two longitudinal spectra in the first and second order approximations together with the three spin-wave spectra of Eq. (15) in Fig. 4 near the magnetic wavevector Q for the compound CsNiCl_3 . Our numerical result for the energy gap of the lower longitudinal mode L_- at Q is $0.96(2J)$ in the first order approximation in Eq. (28). After including the second order terms the energy gap value is now $(0.49)2J$, in agreement with the experimental results of $0.41(2J)$. We also notice that the upper mode L_+ is higher than the L_- mode by about $(0.092)2J$ at Q . We also plot the L_- mode along the path $Q'K'P'QL'O'$ of the hexagonal Brillouin zone in Fig. 5 together with the spin-wave y and zx_- modes. As can be seen, the longitudinal mode is nearly flat over the whole spectrum.

For the compound RbNiCl_3 also with $s = 1$, using the exchange parameters $J = 0.485$ and $J' = 0.0143$ THz with a larger ratio $\xi = J'/J = 0.0295$ [52], we obtain similar longitudinal modes as those of CsNiCl_3 . The numerical result for the energy gap of the L_- mode is 1.16 THz in the first order approximation and 0.69 THz after including the second order contributions at the magnetic wavevector. This later result is in better agreement with the experimental result of about 0.51 THz. We like to point out that there is some difficulty in fitting of Affleck's model with the experimental results for RbNiCl_3 [15, 52].

Finally we turn to the longitudinal modes for the non-integer-spin quasi-1D hexagonal systems. The superexchange interactions in the hexagonal compound CsMnI_3 can be described by the Hamiltonian of (1) with spin quantum number $s = 5/2$ and the nearest-neighbor coupling constants $J = 0.198$ and $J' = 0.001$ THz and negligible anisotropy [30]. This system is very close to the pure 1d system with a very small ratio $\xi = J'/J \approx 0.005$. The linear spin-wave theory may be a poor approximation for such a system. Nevertheless, with a similar analysis as before based on the spin-wave ground state, we obtain the L_- mode energy gap value of 0.64 THz at the magnetic wavevector Q in the first order

approximation, and of 0.47 THz after including the second order contributions. This later value is still much larger than the experimental value of about 0.1 THz by Harrison *et al* [30], which was used to fit a modified spin-wave theory by Plumer and Cailé [18]. Clearly, for such systems as CsMnI_3 , we need a better ground state than that of the spin-wave theory in our analysis.

IV. DISCUSSION

In this paper, we have investigated the excitation states of the quasi-1D hexagonal systems as modeled by the anisotropic Heisenberg Hamiltonian with only the nearest-neighbor couplings. We have obtained the three spin-wave modes and two longitudinal modes. The energy gaps due to the anisotropy and the energy gaps of the longitudinal modes at the magnetic wavevector are investigated and compared with the experimental results for several quasi-1D hexagonal compounds. We have also estimated the higher-order contributions in the large- s expansions for the longitudinal energy spectra. We like to emphasize that our analysis applies to both integer and non-integer spin systems and there are no other fitting parameters than the nearest-neighbor coupling constants and the anisotropy parameter in the model Hamiltonian provided by experiments. Therefore, the good agreement for the longitudinal energy gap values between our calculations and the experimental measurements for the compounds CsNiCl_3 and RbNiCl_3 are particularly satisfactory. The compound CsMnI_3 is very close to the pure 1d model (i.e., ξ very small) for which the spin-wave ground state is not reliable. It is therefore not surprising to find big discrepancy between our estimate based on spin-wave ground state and the experimental result even after including the higher-order contributions in our calculations. Further improvement may be found on two fronts. Firstly, the contribution of the cubic term may be calculated by a perturbation theory in a similar fashion as employed in Ref. [26, 53]. Secondly, a better ground state is needed, particularly for the compound CsMnI_3 where the interchain coupling is particularly weak. A more sophisticated many-body theory such as the coupled-cluster method, particularly its recent variational version [51, 54], may provide such an improvement.

-
- [1] F. D. M. Haldane, Phys. Rev. Lett. **50**, 1153 (1983).
 - [2] D. A. Tennant, R. A. Cowley, S. E. Nagler, and A. M. Tsvetlik, Phys. Rev. B **52**, 13368 (1995).
 - [3] G. Müller, H. Thomas, H. Beck, and J. C. Bonner, Phys. Rev. B **24**, 1429 (1981).
 - [4] W. J. L. Buyers *et al.*, Phys. Rev. Lett. **56**, 371 (1986); R. Morra, Phys. Rev. B **38**, 543 (1988); Z. Tun, W. J. L. Buyers, R. L. Armstrong, K. Hirakawa, and B. Briat, Phys. Rev. B **42**, 4677 (1990).
 - [5] L. P. Regnault, I. Zaliznyak, J. P. Renard, and C. Vettier, Phys. Rev. B **50**, 9174 (1994).
 - [6] S. Ma, C. Broholm, D. H. Reich, B. J. Sternlieb, and R. W. Erwin, Phys. Rev. Lett. **69**, 3571 (1992); Phys. Rev. B **51**, 3289 (1995).
 - [7] M. Steiner, K. Kakurai, J. K. Kjems, D. Petitgrand, and R. Pynn, J. Appl. Phys. **61**, 3953 (1987); I. A. Zaliznyak, L.-P. Regnault, and D. Petitgrand, Phys. Rev. B **50**, 15824 (1994); I. A. Zaliznyak, S.-H. Lee, and S. V. Petrov, Phys. Rev. Lett. **87**, 17202 (2001).
 - [8] M. Kenzelmann *et al.*, Phys. Rev. Lett. **87**, 017201 (2001); M. Kenzelmann *et al.*, Phys. Rev. B **66**, 024407 (2002).
 - [9] E. S. Sørensen and I. Affleck, Phys. Rev. B **49**, 13235 (1994).

- [10] O. Golinelli, T. Jolicoeur, and R. Lacaze, *Phys. Rev. B* **46**, 10854 (1992).
- [11] S. Yamamoto, *Phys. Rev. Lett.* **75**, 3348 (1995).
- [12] J. Deisz, M. Jarrell, and D. L. Cox, *Phys. Rev. B* **48**, 10227 (1993).
- [13] M. Takahashi, *Phys. Rev. Lett.* **62**, 2313 (1989); M. Takahashi, *Phys. Rev. B* **48**, 311 (1993).
- [14] I. Affleck, *Phys. Rev. Lett.* **62**, 474 (1989); *Phys. Rev. Lett.* **65**, 2477 (1990); *Phys. Rev. Lett.* **65**, 2835 (1990).
- [15] I. Affleck and G. F. Wellman, *Phys. Rev. B* **46**, 8934 (1992).
- [16] M. Enderle, Z. Tun, W. J. L. Buyers, and M. Steiner, *Phys. Rev. B* **59**, 4235 (1999).
- [17] T. Ohyama and H. Shiba, *Journal of the Physical Society of Japan* **62**, 3277 (1993).
- [18] M. L. Plumer and A. Caillé, *Phys. Rev. Lett.* **68**, 1042 (1992).
- [19] B. Lake, D. A. Tennant, and S. E. Nagler, *Phys. Rev. B* **71**, 134412 (2005).
- [20] H. J. Schulz, *Phys. Rev. Lett.* **77**, 2790 (1996).
- [21] F. H. L. Essler, A. M. Tsvelik, and G. Delfino, *Phys. Rev. B* **56**, 11001 (1997).
- [22] C. Rüegg *et al.*, *Phys. Rev. Lett.* **100**, 205701 (2008).
- [23] Y. Xian, *Phys. Rev. B* **74**, 212401 (2006).
- [24] Y. Xian, *Journal of Physics: Condensed Matter* **19**, 216221 (2007).
- [25] R. P. Feynman, *Phys. Rev.* **94**, 262 (1954).
- [26] R. P. Feynman and M. Cohen, *Phys. Rev.* **102**, 1189 (1956).
- [27] Y. Xian, *Journal of Physics: Condensed Matter* **23**, 346003 (2011).
- [28] A. Sorgen, E. Cohen, and J. Makovsky, *Phys. Rev. B* **10**, 4643 (1974).
- [29] M. C. Rheinstädter, M. Enderle, and G. J. McIntyre, *Phys. Rev. B* **70**, 224420 (2004).
- [30] A. Harrison, M. F. Collins, J. Abu-Dayyeh, and C. V. Stager, *Phys. Rev. B* **43**, 679 (1991).
- [31] M. Merdan and Y. Xian, *Journal of Low Temperature Physics*, DOI 10.1007/s10909-012-0778-1 (2012).
- [32] P. Santini, G. Fath, Z. Domanski, and P. Erdos, *Phys. Rev. B* **56**, 5373 (1997).
- [33] P. Santini, Z. Domanski, J. Dong, and P. Erdos, *Phys. Rev. B* **54**, 6327 (1996).
- [34] T. Delica, W. J. M. de Jonge, K. Kopinga, H. Leschke, and H. J. Mikeska, *Phys. Rev. B* **44**, 11773 (1991).
- [35] M. Baehr *et al.*, *Phys. Rev. B* **54**, 12932 (1996).
- [36] E. Rastelli and A. Tassi, *Phys. Rev. B* **49**, 9679 (1994).
- [37] R. R. P. Singh and D. A. Huse, *Phys. Rev. Lett.* **68**, 1766 (1992).
- [38] S. J. Miyake, *Journal of the Physics Society Japan* **61**, 983 (1992).
- [39] A. V. Chubukov, S. Sachdev, and T. Senthil, *Journal of Physics: Condensed Matter* **6**, 8891 (1994).
- [40] A. Chernyshev and M. Zhitomirsky, *Physical Review B* **79**, 144416 (2009).
- [41] I. Affleck, *Phys. Rev. Lett.* **65**, 2835 (1990).
- [42] K. Kakurai, M. Steiner, R. Pynn, and J. K. Kjems, *Journal of Physics: Condensed Matter* **3**, 715 (1991).
- [43] R. Feile *et al.*, *Solid State Communications* **50**, 435 (1984).
- [44] D. Welz, *Journal of Physics: Condensed Matter* **5**, 3643 (1993).
- [45] S.M. Girvin, A.H. MacDonald, and P.M. Platzman, *Phys. Rev. B* **33**, 2481 (1986).
- [46] F. Coester and H. Kümmel, *Nuclear Physics* **17**, 477 (1960).
- [47] J. Cizek, *The Journal of Chemical Physics* **45**, 4256 (1966).
- [48] R. F. Bishop, *Theoretica Chimica Acta* **80**, 95 (1991).
- [49] K. Emrich, *Nuclear Physics A* **351**, 379 (1981).
- [50] R. F. Bishop, J. B. Parkinson, and Y. Xian, *Phys. Rev. B* **43**, 13782 (1991).
- [51] Y. Xian, *Phys. Rev. B* **66**, 184427 (2002); **72**, 224438 (2005).
- [52] Z. Tun, W. J. L. Buyers, A. Harrison, and J. A. Rayne, *Phys. Rev. B* **43**, 13331 (1991).
- [53] H.W. Jackson and E. Feenberg, *Rev. Mod. Phys.* **34**, 686 (1962).
- [54] Y. Xian, *Phys. Rev. A* **77**, 042103 (2008).